

**ARTICLE**

# A novel integrated QSP model of in vivo human glucose regulation to support the development of a glucagon/GLP-1 dual agonist

Rolien Bosch<sup>1</sup> | Marcella Petrone<sup>2</sup> | Rosalin Arends<sup>3</sup> | Paolo Vicini<sup>2</sup> |  
Eric J. G. Sijbrands<sup>4</sup> | Sven Hoefman<sup>1</sup> | Nelleke Snelder<sup>1</sup>

<sup>1</sup>LAP&P Consultants, Leiden, The Netherlands

<sup>2</sup>Clinical Pharmacology and Safety Sciences, AstraZeneca, Cambridge, UK

<sup>3</sup>AstraZeneca, Gaithersburg, Maryland, USA

<sup>4</sup>Department of Internal Medicine, Erasmus MC, University Medical Center, Rotterdam, The Netherlands

**Correspondence**

Rolien Bosch, LAP&P Consultants, Archimedesweg 31, Leiden, The Netherlands.  
Email: r.bosch@lapp.nl

**Present address**

Paolo Vicini, Confo Therapeutics, Gent, Belgium

**Funding information**

No funding was received for this work

**Abstract**

Glucagon-like peptide-1 (GLP-1) receptor agonists (GLP-1RAs) and dual GLP-1/glucagon receptor agonists improve glycaemic control and cause significant weight loss in patients with type 2 diabetes.<sup>1</sup> These effects are driven in part by augmenting glucose-stimulated insulin release (incretin effect), reducing caloric intake and delayed gastric emptying. We developed and externally validated a novel integrated quantitative systems pharmacology (QSP) model to gain quantitative insight into the relative contributions and mechanisms of drugs modulating glucose regulatory pathways. This model (4GI model) incorporates known feedback mechanisms among glucose, GLP-1, glucagon, glucose-dependent insulinotropic peptide (GIP), and insulin after glucose provocation (i.e., food intake) and drug intervention utilizing published nonpharmacological and pharmacological (liraglutide, a GLP-1RA) data. The resulting model accurately describes the aforementioned mechanisms and independently predicts the effects of the GLP-1RAs (dulaglutide and semaglutide) on system dynamics. Therefore, the validated 4GI model represents a quantitative decision-making tool to support the advancement of novel therapeutics and combination strategies modulating these pathways.

**Study Highlights****WHAT IS THE CURRENT KNOWLEDGE ON THE TOPIC?**

Mechanistic pharmacokinetic/pharmacodynamic (PK/PD) models are available to quantify drug effects on glucose, insulin, and glucagon-like peptide-1 (GLP-1) dynamics in humans. However, the integrated relationships between these biomarkers, glucose-dependent insulinotropic peptide (GIP), and glucagon are not captured by these models.

**WHAT QUESTION DID THIS STUDY ADDRESS?**

First, the purpose of this study was to develop a quantitative systems pharmacology (QSP) model that could integrate the dynamics of glucose, insulin, GLP-1,

This is an open access article under the terms of the Creative Commons Attribution-NonCommercial-NoDerivs License, which permits use and distribution in any medium, provided the original work is properly cited, the use is non-commercial and no modifications or adaptations are made.

© 2021 The Authors. *CPT: Pharmacometrics & Systems Pharmacology* published by Wiley Periodicals LLC on behalf of American Society for Clinical Pharmacology and Therapeutics.

glucagon, and GIP with the effects of drugs on the system. Second, we assessed the predictive power of the model by external validation with other GLP-1 agonists (dulaglutide and semaglutide) data.

#### **WHAT DOES THIS STUDY ADD TO OUR KNOWLEDGE?**

The model quantitatively describes the opposing insulin and glucagon effects as well as the incretin effects on glucose homeostasis in fasting, fed, untreated, and treated with GLP-1RA states.

#### **HOW MIGHT THIS CHANGE DRUG DISCOVERY, DEVELOPMENT, AND/OR THERAPEUTICS?**

The 4GI model is a quantitative decision-making tool supporting the progression of novel molecules intended to modulate multiple glucose regulation pathways, including GLP-1RA. It can improve our understanding of the mechanism of actions of new candidate drugs.

## **INTRODUCTION**

Type 2 diabetes mellitus (T2DM) is a chronic disease characterized by elevated blood glucose levels, occurring from a relative deficiency in circulating insulin levels on the background and reduced insulin action. Glucagon-like peptide-1 receptor agonists (GLP-1Ras) represent an attractive class of antidiabetic drugs based on effects on improving glycemic control while reducing body weight.<sup>1</sup> Reduction in body weight (typically  $\geq 5\%$  of body weight) not only improves glycemic control, but is also associated with slowing or reversing disease progression, reducing cardiovascular risk, and mortality rates.<sup>2,3</sup>

GLP-1 is an incretin peptide hormone secreted by enteroendocrine cells of the small intestine following food intake. GLP-1, and analogs of native GLP-1, improve glucose control with a low risk of hypoglycemia by inducing glucose-stimulating insulin release, delaying gastric emptying, and suppressing glucagon secretion. Additionally, GLP-1RAs effects on delayed gastric emptying and increased satiety lead to induction of body weight loss.

Glucagon is a peptide hormone secreted by pancreatic islet  $\alpha$  cells and involved with regulating blood levels of glucose in the fasting state to prevent hypoglycemia. The hyperglycemic action of glucagon is mediated by increased hepatic glycogenolysis and gluconeogenesis, thereby increasing endogenous glucose production. It was also found that glucagon can inhibit food intake and may increase energy expenditure, providing a rationale for the use of glucagon for weight loss, although the mechanism of action is still unclear.<sup>1</sup> Glucagon has also been shown to have an effect on lipid metabolism through inhibition of lipogenesis and stimulation of lipolysis.<sup>4,5</sup>

Oxyntomodulin (OXM) is an endogenous peptide that has activity at both the GLP-1 and glucagon receptors. OXM has been shown to reduce food intake, glucose levels,

and body weight preclinically and in humans.<sup>6,7</sup> The circulatory half-life of OXM is short (less than 10 min), leading to development of GLP-1/glucagon receptor dual agonists with improved properties, for the potential treatment of T2DM, obesity, and nonalcoholic steatohepatitis (NASH).

Cotadutide is a novel synthetic, lipidated, long-acting peptide with GLP-1 and glucagon receptor dual agonism activity that is currently in clinical development as a potential treatment for overweight and obese individuals with T2DM and NASH.<sup>8-10</sup> Preclinical data has shown that, in obese insulin-resistant mice and lean mice treated with cotadutide, the balance of agonism at both the GLP-1 and glucagon receptors provides glycemic control following a glucose challenge without an adverse effect on fasting glucose levels.<sup>11</sup> Subchronic treatment of cotadutide leads to body weight loss in obese mice and in non-human primates, and has shown efficacy in mouse models of NASH.<sup>4</sup>

Given the complexity of such a dual mechanism of action, novel quantitative approaches are needed to aid the in vivo prediction of the combined actions of GLP-1/glucagon dual-agonists on glucose homeostasis, and more in general to characterize simultaneous modulation of several steps in the complex regulatory cascade of glucose control, either through multiple action or combinations of drugs.

Mechanistic pharmacokinetic/pharmacodynamic (PK/PD) models that quantify drug effects on glucose, insulin, and GLP-1 dynamics in humans are available.<sup>12-14</sup> However, the integrated relationships among glucose, insulin, GLP-1, glucagon, and glucose-dependent insulinotropic peptide (GIP) dynamics are not captured by these models. Here, we describe the development of a novel quantitative systems pharmacology (QSP) model that characterizes the inter-relationship among glucose, GLP-1, glucagon, GIP, and insulin (4GI model), which can be used to predict the action of GLP-1/glucagon dual-agonists on glucose homeostasis.

## METHODS

### Data

We developed the QSP model to quantitate the relationship among glucose, GLP-1, glucagon, GIP, and insulin using published clinical data during and after pharmacological and nonpharmacological challenges used to perturb glucose-regulated pathways. It was hypothesized that the parameters of the system could be identified in a drug-independent manner by perturbing multiple parts of the system with a variety of challenges nonpharmacological challenges, for example, glucose, GLP-1, glucagon, and GIP challenges. This would enable the QSP model to describe the effects of drugs targeting or affecting the glucose-regulatory system in a manner similar to nonpharmacological challenges. Liraglutide was used to inform the model on the mechanistic effects of a GLP-1RA on the system, to enable extrapolation, and predict the long-term effects of GLP-1RA. To validate the QSP model, published effects of dulaglutide and semaglutide on glucose control were compared to model-predicted effects. An overview of the selected data is shown in Table 1 and Supplementary S1.

### Data extraction

Data were extracted from publications using the program DigitizeIt.<sup>15</sup> Study meals were accounted for by adding meal dosing records to the dataset as glucose amounts. If meal size information was available, this was used to calculate the amount of glucose. In case no information was provided, a standard meal of 75 g of glucose was assumed, regardless of the type of meal (e.g., breakfast, lunch, dinner, and evening snack) and the amount of glucose entering the system was accounted for by estimation of the hypothetical glucose bioavailability per study and meal type.

### Compound potency assay and free fraction

To determine the half maximal effective concentration ( $EC_{50}$ ) of GLP-1, glucagon, liraglutide, semaglutide, and dulaglutide, a GLP-1 Receptor Activation Assay was used (unpublished data), based on the elevation of cyclic adenosine monophosphate (cAMP) production in Chinese hamster ovary (CHO) cells that express the human GLP-1 receptor. The  $EC_{50}$  values were determined in the absence of serum albumin to reflect the potency of the free compound. The results from this assay were assumed to mirror in vivo potency.

Plasma free fractions were measured in-house, except for liraglutide plasma free fraction which was obtained

from literature.<sup>16</sup> Table 2 shows the  $EC_{50}$  values and free fraction information used in the 4GI model.

### Model development

The integrated glucose-insulin (IGI) model by Silber et al.<sup>12,17</sup> in combination with knowledge from the Landersdorfer model,<sup>14</sup> in particular the description of the incretin effect, was used as a starting point for model development. Glucose and insulin disposition parameters were fixed to the published values.<sup>12,13</sup> The model was adjusted and extended to describe glucagon, GLP-1, and GIP dynamics. Plasma liraglutide, dulaglutide, and semaglutide concentrations were predicted using published PK models<sup>18–20</sup>

Because the data sets only provided population means, interindividual variability was not taken into account during model development, which means that all model predictions are typical value predictions.

### Model validation

The model was validated using the glucose data extracted from the dulaglutide arms of the AWARD-6 study<sup>21</sup> and the dulaglutide and semaglutide arms of the SUSTAIN-7 study.<sup>22</sup> For each treatment arm, 1000 profiles were simulated taking into account parameter uncertainty. Visual agreement between simulated and observed profiles was used to assess suitability of model performance.

The schematic overview of the 4GI model is presented in Figure 1. The NONMEM code for the final model is provided in Appendix S1.

### Model description

#### Meal intake

Oral glucose or meal consumption was modeled via a glucose dosing compartment mimicking the stomach, followed by a buffer compartment reflecting the intestine through which glucose is absorbed into the central compartment. From the glucose buffer compartment, glucose can also enter further into the gut, described by three serial glucose transit compartments, and subsequently leave the system.

#### Glucose dynamics

The glucose portion of the model is a two-compartment disposition model with elimination from the central

TABLE 1 Selection of data included in this study

Publication	Subjects	Challenge/compound administration	Biomarkers	Time course
Development dataset				
Silber 2007 <sup>12</sup>	HV and T2DM patients	IVGTT and IVGTT + insulin	Glucose, insulin	5 h
Jauslin 2011 <sup>13</sup>	T2DM patients	Meal	Glucose, insulin	24 h
Landersdorfer 2011 <sup>14</sup>	T2DM patients	Meal	Glucose, insulin, GLP-1	24 h
Tan 2012 <sup>27</sup>	Healthy obese volunteers	i.v. GLP-1 and/or glucagon	Glucose, insulin, GLP-1, glucagon	2 h
Edholm 2010 <sup>32</sup>	HV	Meal and GLP-1 or GIP i.v.	GLP-1, glucagon, GIP	3 h
Vilsbøll 2006 <sup>24</sup>	HV and T2DM patients	GIP i.v.	GIP	1 h
Vilsbøll 2002 <sup>29</sup>	HV and obese T2DM patients	Glucose and GLP-1 or GIP or placebo i.v.	Glucose, insulin, GLP-1, glucagon, GIP	4 h
Larsen 2001 <sup>44</sup>	T2DM patients	Meal and GLP-1	Glucose, insulin, glucagon	24 h
Schneek 2013 <sup>26</sup>	T2DM patients	Meal	Glucose, insulin, glucagon	24 h
Camstra 2013 <sup>30</sup>	T2DM and healthy obese	Meal	Glucose, insulin, GLP-1, glucagon, GIP	5 h
LEAD-3 <sup>45</sup>	T2DM patients	Meal + liraglutide	Glucose	52 weeks
LEAD-6 <sup>46</sup>	T2DM patients	Meal + liraglutide	Glucose	40 weeks
AWARD-6 <sup>21</sup>	T2DM patients	Meal + liraglutide	Glucose	26 weeks
Validation dataset				
AWARD-6 <sup>21</sup>	T2DM patients	Meal + dulaglutide	Glucose	26 weeks
SUSTAIN-7 <sup>22</sup>	T2DM patients	Meal + dulaglutide or semaglutide	Glucose	40 weeks

Abbreviations: GLP, glucagon-like peptide; HV, healthy volunteer; IVGTT, intravenous glucose tolerance test; T2DM, Type-2 diabetes mellitus.

Compound	GLP-1 receptor EC <sub>50</sub> (pM)	Glucagon receptor EC <sub>50</sub> (pM)	Free fraction (%)
GLP-1(7-36)NH1	1.92 <sup>a</sup>		
Glucagon		1.54 <sup>a</sup>	
Liraglutide	6 <sup>a</sup>		0.51 <sup>47</sup>
Dulaglutide	80 <sup>a</sup>		100 <sup>48</sup>

**TABLE 2** EC<sub>50</sub> and free fraction information used

<sup>a</sup>Unpublished in-house data.

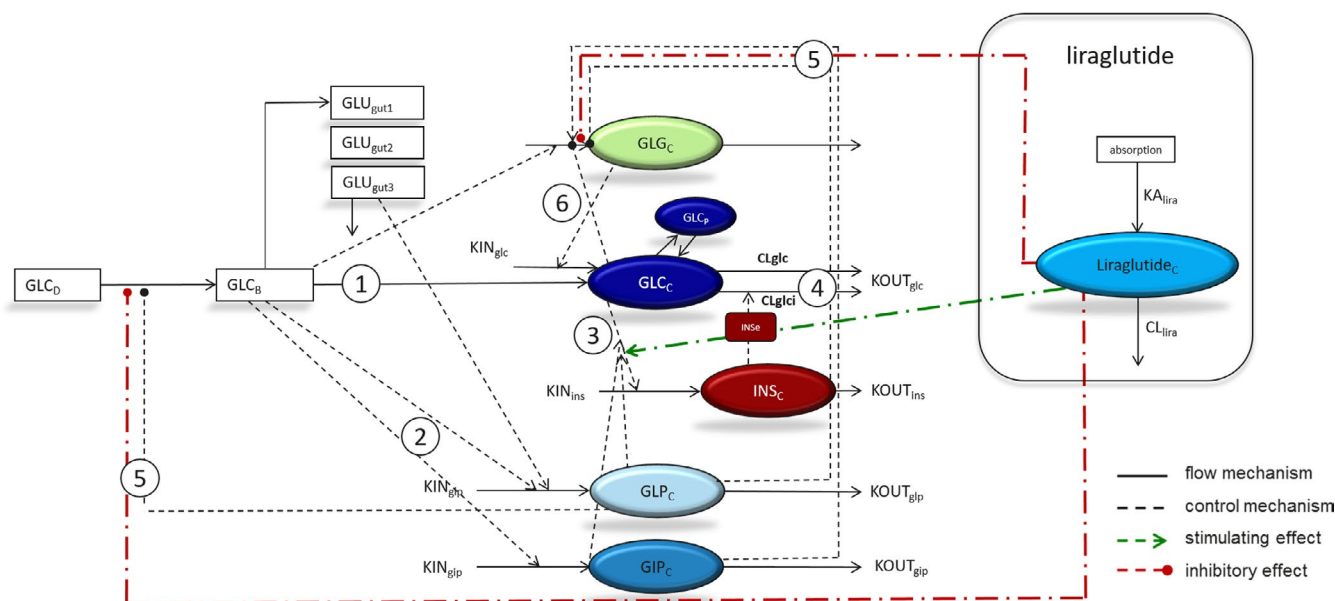


**FIGURE 1** Schematic overview of the model. Schematic overview of the 4GI model. 1. Upon meal intake, glucose enters the system via the stomach (glucose dosing GLC<sub>D</sub>) moving into the intestines (glucose buffer GLC<sub>B</sub>) from which it can either go further into the intestines (glucose gut GLU<sub>gut</sub>) and get cleared or being absorbed into the blood stream, represented by the central glucose compartment (GLC<sub>C</sub>), and distributed over the peripheral compartment (GLC<sub>P</sub>). 2. Food intake increases incretin hormones GLP-1 and GIP. Food intake also increases glucagon levels. 3. Due to the increase in glucose, insulin levels rise, this is enhanced by GLP-1 and GIP (the incretin effect). 4. Insulin increases glucose elimination. 5. Other incretin hormone effects are, decreasing gastric emptying (GLP-1), decreasing glucagon levels (GLP-1), or increasing glucagon levels (GIP). 6. Glucose decreases glucagon secretion, whereas glucagon stimulates glucose production to keep glucose levels from dropping too low and avoid hypoglycemia. Liraglutide has the same effects on the system as the endogenous GLP-1 (e.g., stimulation of glucose-dependent insulin secretion, inhibition of glucagon secretion and inhibition of glucose absorption)

compartment that was split between insulin-dependent and insulin-independent elimination (CL<sub>glci</sub> [L/h/pmol] and CL<sub>glc</sub> [L/h], respectively), with endogenous production of glucose (EGP represented here as KIN<sub>glc</sub> [mmol/h]) entering the central compartment. Disposition parameters (CL<sub>glci</sub>, CL<sub>glc</sub>, Q<sub>glc</sub>, VC<sub>glc</sub>, and VP<sub>glc</sub>) for healthy volunteers (HVs) as well as patients with T2DM were fixed to published values<sup>12,13</sup> and kept fixed throughout model development (Table 3). The rate constant between the glucose dosing and buffer compartment (representing gastric emptying), as well as that between the buffer and central glucose compartment, are described by the absorption rate constants K<sub>Aglc2</sub> (/h) and K<sub>Aglc</sub> (/h), respectively. K<sub>Aglc2</sub> is influenced by GLP-1, with GLPGLC<sub>AI</sub> being

the inhibiting GLP-1 effect (1 being complete, 100% inhibition) on glucose absorption (Equation 1):

$$K_{Aglc2} = K_{Aglc} * (1 - GLPGLC_{AI}) \quad (1)$$

A maximum effect (E<sub>max</sub>) function describes the GLP-1 effect on glucose absorption as a function of concentration (Equation 2), where <sub>AI</sub> stands for absorption inhibition.

$$GLPGLC_{AI} = E_{MAX\_2} * \frac{\left(\frac{C_{glp}}{EC50_2}\right)^{HILL\_2}}{\left(1 + \left(\frac{C_{glp}}{EC50_2}\right)^{HILL\_2}\right)} \quad (2)$$

**TABLE 3** Final estimates (PK parameters)

<b>Glucose, insulin, GLP-1, glucagon, and GIP PK parameters</b>			
	<b>Parameter description</b>	<b>Estimate</b>	<b>RSE (%)</b>
<b>Glucose disposition parameters</b>			
CL <sub>glc</sub> , L/h T2DM	Glucose clearance T2DM	1.72	Fixed
CL <sub>glc</sub> , L/h HV	Glucose clearance HV	5.36	Fixed
CL <sub>glci</sub> , L/h/pmol/L T2DM	Insulin-dependent glucose clearance T2DM	0.0256	Fixed
CL <sub>glci</sub> , L/h/pmol/L HV	Insulin-dependent glucose clearance HV	0.072	Fixed
Q <sub>glc</sub> , L/h	Intercompartmental clearance of glucose	26.5	Fixed
VC <sub>glc</sub> , L	Glucose volume of distribution central compartment	9.33	Fixed
VP <sub>glc</sub> , L	Glucose volume of distribution peripheral compartment	8.56	Fixed
KA <sub>glc</sub> , 1/h	Glucose absorption rate constant	0.853	14.1
Ke <sub>glc</sub> , 1/h	Transit rate constant glucose in gut	0.281	24.5
Ke <sub>glc</sub> , 1/h	Rate constant glucose from buffer to central compartment	1.93	15.3
<b>Insulin disposition parameters</b>			
CL <sub>ins</sub> , L/h	Insulin clearance	73.2	Fixed
VC <sub>ins</sub> , L	Insulin volume of distribution central compartment	6.09	Fixed
Ke <sub>0ins</sub> , 1/h	Rate constant effect compartment insulin on glucose clearance	0.85	27.0
<b>GLP-1 disposition parameters</b>			
VC <sub>glp</sub> , L	GLP-1 volume of distribution central compartment	16	29.3
VM <sub>GLP</sub> , pmol/L*h	GLP-1 maximum concentration dependent clearance	2893	7.41
KM <sub>GLP</sub> , pmol/L	Concentration at half maximum clearance	136	10.3
Factor total GLP	Factor for total GLP-1 measurements	3.8	16.9
<b>Glucagon disposition parameters</b>			
CL <sub>glg</sub> , L/h	Glucagon clearance	453	5.55
VC <sub>glg</sub> , L	Glucagon volume of distribution central compartment	64.6	11.7
<b>GIP disposition parameters</b>			
CL <sub>gip</sub> , L/h	GIP clearance	86.8	Fixed
VC <sub>gip</sub> , L	GIP volume of distribution central compartment	9.21	Fixed
Q <sub>gip</sub> , L/h	GIP intercompartmental clearance	49.4	Fixed
VP <sub>gip</sub> , L	GIP volume of distribution peripheral compartment	22.8	Fixed
<b>Residual Error</b>			
Glucose	Proportional residual error glucose	0.0211	27.5
Insulin	Proportional residual error insulin	0.305	38.4
GLP-1	Proportional residual error GLP-1	0.0602	36.0
Glucagon	Proportional residual error glucagon	0.0348	27.4
GIP	Proportional residual error GIP	0.109	32.6

Note: Estimated and fixed PK parameters. The relative standard error RSE (%) is calculated as the standard error SE/estimate\*100.

Abbreviations: GIP, glucose-dependent insulinotropic peptide; GLP, glucagon-like peptide; HV, healthy volunteer; PK, pharmacokinetic; RSE, relative standard error; T2DM, type 2 diabetes mellitus.

Glucose dynamics (mmol/h) in the glucose central compartment are described by (Equation 3).

$$\begin{aligned} \frac{dGLC_C(t)}{dt} = & KA_{glc} * GLC_B(t) + KIN_{glc} * g_{lgEFFglc} \\ & - K27 * GLC_C(t) + K72 * GLC_P(t) - \left( \frac{CL_{glc}}{VC_{glc}} \right) \\ & * GLC_C(t) - \left( \frac{CL_{glci} * INS_E(t)}{VC_{glc}} \right) * GLC_C(t) \end{aligned} \quad (3)$$

with  $GLC_B$ ,  $GLC_C$  and  $GLC_P$  being the amount (mmol) of glucose in the buffer, central and peripheral compartments, respectively.  $K27$  (/h) and  $K72$  (/h) represent the rate constants for glucose distribution from and to the peripheral compartment. Insulin influences the insulin-dependent glucose clearance via an effect compartment ( $INS_E$ , [pmol/L]).

$KIN_{glc}$  is the basal endogenous glucose production, and its value is derived from the steady-state conditions (Equation 4).



$$\text{KINglc} = \text{BSLglc} * (\text{CLglc} + \text{CLglci} * \text{BSLins}) \quad (4)$$

Glucose production over time was influenced by glucagon (glgEFFglc) via a Hill  $E_{\max}$  relationship, and is corrected for the baseline effect, such that glgEFFglc equals 1 at steady-state (Equations 5, 6, 7).

$$\text{glgEFFglc} = \frac{1 + \text{GLGGLC}_S}{1 + \text{GLGGLC}_{S0}} \quad (5)$$

$$\text{GLGGLC}_{S0} = \text{EMAX}_4 * \frac{\left(\frac{\text{BSLglg}}{\text{EC50}_4}\right)^{\text{HILL}_4}}{\left(1 + \left(\frac{\text{BSLglg}}{\text{EC50}_4}\right)^{\text{HILL}_4}\right)} \quad (6)$$

$$\text{GLGGLC}_S = \text{EMAX}_4 * \frac{\left(\frac{\text{Cglg}}{\text{EC50}_4}\right)^{\text{HILL}_4}}{\left(1 + \left(\frac{\text{Cglg}}{\text{EC50}_4}\right)^{\text{HILL}_4}\right)} \quad (7)$$

GLGGLC<sub>S0</sub> describes the baseline (steady-state) effect of glucagon on glucose, with BSLglg (pmol/L) being the glucagon baseline. GLGGLC<sub>S</sub> is the effect on glucose production, which depends on the dynamic glucagon concentration (Cglg, [pmol/L]). Model parameters with <sub>S</sub> denote a stimulatory effect; <sub>I</sub> stands for an inhibitory effect. EMAX<sub>4</sub> (1/pM) is the maximum effect of glucagon on glucose production, and EC50<sub>4</sub> is the concentration (pmol/L) at which 50% of the maximum effect is reached. HILL<sub>4</sub> is the Hill coefficient that defines the shape of the relationship.

## Insulin dynamics

The model for insulin is a one-compartment disposition model with elimination from the central compartment, as described by (Equation 8):

$$\frac{d\text{INS}_c(t)}{dt} = \text{KINins} * (1 + \text{STglc} * \text{Cglc}(t)^{\text{GLCINS}_S}) - \frac{\text{CLins}}{\text{VCins}} * \text{INS}_c(t). \quad (8)$$

with VCins (L) being the volume of distribution of the central insulin compartment and CLins (L/h) the insulin clearance from the central compartment. VCins and CLins were fixed to literature values.<sup>12,13</sup>

Insulin production (KINins [pmol/h]) at baseline is in equilibrium with insulin elimination (Equation 9).

$$\text{KINins} = \text{BSLins} * \frac{\text{CLins}}{(1 + \text{STglc0} * \text{BSLglc})^{\text{GLCINS}_S}}. \quad (9)$$

where BSLins (pmol/L) is the insulin concentration at baseline. Changes in glucose concentrations influence the insulin production flux, and GLCINS<sub>S</sub> (1/mM) is the stimulating effect of glucose on insulin production. This glucose-dependent insulin secretion is stimulated by GLP-1 and GIP concentrations (STglc; Equations 10, 11, 12). These effects are also known as the incretin effects.

$$\text{STglc} = \text{GLPINS}_S + \text{GIPINS}_S \quad (10)$$

$$\text{GLPINS}_S = \text{EMAX}_1 * \frac{\left(\frac{\text{Cglp}}{\text{EC50}_1}\right)^{\text{HILL}_1}}{\left(1 + \left(\frac{\text{Cglp}}{\text{EC50}_1}\right)^{\text{HILL}_1}\right)}. \quad (11)$$

$$\text{GIPINS}_S = \text{Cgip}^{\text{POW}_3} \quad (12)$$

In these equations, Cglp (pmol/L) and Cgip (pmol/L) represent the endogenous GLP-1 and GIP concentration, respectively, and EMAX<sub>1</sub> (1/pM) is the maximal GLP effect on glucose-dependent insulin secretion. The EC50<sub>1</sub> (pmol/L) is the concentration of endogenous GLP-1 at 50% of maximum effect. POW<sub>3</sub> describes the shape of the GIP on the glucose-dependent insulin secretion relationship.

## GLP-1 dynamics

GLP-1 (active form) distribution kinetics are described by a one-compartment model with a Michaelis Menten (saturable) clearance from the central compartment (Equations 13, 14) Vilsbøll et al.<sup>23</sup>

$$\frac{\text{GLP}_C(t)}{dt} = \text{KINglp} * (1 + \text{FDGLP}_S) * (1 + \text{FDGLP}_{S2}) - \frac{\text{VM} * \text{C}_{\text{glp}}(t)}{(\text{KM} + \text{C}_{\text{glp}}(t))}. \quad (13)$$

$$\text{KINglp} = \frac{\text{VM} * \frac{\text{BSLglp}}{\text{VCglp}}}{\text{KM} + \text{BSLglp}}. \quad (14)$$

KINglp is the GLP-1 production at baseline, as derived from steady-state conditions, and BSLglp [pmol/L] is the GLP-1 concentration at baseline.

KINglp is influenced by food intake from the buffer (FDGLP<sub>S</sub>) and transit gut compartments (FDGLP<sub>S2</sub>, [1/pM]; Equations 15 and 16).

$$\text{FDGLP}_S = \text{FDGLP} * \text{GLC}_B(t) \quad (15)$$

$$\text{FDGLP}_{S2} = \text{FDGLP2} * \text{GLC}_{\text{gut3}}(t) \quad (16)$$

FDGLP and FDGLP2 are the slopes of the linear effects, and  $GLC_B(t)$  (mmol) is the glucose amount in the buffer absorption compartment.  $GLC_{gut3}(t)$  (mmol) is the glucose amount in the third glucose gut transit compartment.

## Glucagon dynamics

The glucagon submodel is a one-compartment disposition model (Equation 17).

$$\frac{GLG_C(t)}{dt} = KINGlg * (1 + FDGLP_S) * glcEFFglg * glpEFFglg * gipEFFglg - \left( \frac{CLglg}{VCglg} \right) * GLG_C(t) \quad (17)$$

$KINGlg$  is the glucagon production at baseline (Equation 18), as derived from steady-state conditions.

$$KINGlg = (BSLglg * CLglg) \quad (18)$$

FDGLG\_S (1/pM) is the food effect on glucagon levels, which is described by a linear effect dependent on the amount of glucose in the buffer compartment, with FDGLG (1/pM) being the estimated slope of the effect (Equation 19).

$$FDGLG_S = FDGLG * GLC_B(t) \quad (19)$$

Glucose production is stimulated by glucagon via the  $glcEFFglg$  effect with  $POW_2$  as the estimated power of the effect (Equation 20).

$$glcEFFglg = \left( \frac{BSLglc}{Cglc(t)} \right)^{POW_2} \quad (20)$$

At glucose levels ( $Cglc$ ) equal to or higher than the baseline ( $BSLglc$ ), the effect inhibits glucagon production ( $KINGlg$ ). When glucose drops below baseline, glucagon production is stimulated. The glucagon-stimulating effect at glucose concentrations below baseline could only be estimated for the HV population. For the T2DM population, the effect of glucose on glucagon production at glucose concentrations below baseline could not be estimated and was assumed to be equal to the baseline glucagon on glucose production effect.

The  $glpEFFglg$  is the inhibiting GLP-1 effect on glucagon production (Equations 21, 22, and 23).  $EMAX_3$  (1/pM) is the maximum effect,  $EC50_3$  the half-maximum effect concentration (pmol/L) and  $HILL_3$  defines the shape of the concentration-effect relationship.

$$glpEFFglg = \frac{(1 - GLPGLG_I)}{(1 - GLPGLG_I0)} \quad (21)$$

$$GLPGLG_I0 = EMAX_3 * \frac{\left( \frac{BSLglg}{EC50_3} \right)^{HILL_3}}{\left( 1 + \left( \frac{BSLglg}{EC50_3} \right)^{HILL_3} \right)} \quad (22)$$

$$GLPGLG_I = EMAX_3 * \frac{\left( \frac{Cglg}{EC50_3} \right)^{HILL_3}}{\left( 1 + \left( \frac{Cglg}{EC50_3} \right)^{HILL_3} \right)} \quad (23)$$

The  $gipEFFglg$  is the stimulating effect of GIP on glucagon production and is described by a power model (Equation 24).

$$gipEFFglg = \left( \frac{Cgip}{BSLgip} \right)^{POW_4} \quad (24)$$

## GIP dynamics

The GIP submodel is a two-compartment disposition model described by (Equation 25). The GIP PK parameters ( $CLgip$ ,  $VCgip$ , and  $Qgip$ ) were estimated based on the digitized data from the Vilsbøll 2006 paper<sup>24</sup> and kept fixed during further model optimization.

$$\frac{GIP_C(t)}{dt} = KINGgip * (1 + FDGIP_S) + K126 * GIP_P(t) - K612 * GIP_C(t) - \left( \frac{CLgip}{VCgip} \right) * GIP_C(t) \quad (25)$$

$KINGgip$  is the endogenous GIP production, derived from steady-state conditions (Equation 26).  $GIP_C(t)$  and  $GIP_P(t)$  represents the amount of GIP [pmol] in the central and peripheral compartment over time, respectively.

$$KINGgip = BSLgip * CLgip \quad (26)$$

Where  $CLgip$  (L/h) and  $VCgip$  (L) represent the clearance and central volume of distribution of GIP, and  $K126$  (1/h), and  $K612$  (1/h) represent the rate constants from and to the peripheral compartments.

$FDGIP_S$  (1/pM) is the food effect on GIP, described by a linear increase in GIP following food intake via the glucose buffer compartment (Equation 27), with  $FDGIP$  being the estimated slope of the effect.

$$FDGIP_S = FDGIP * GLC_{buffer}(t) \quad (27)$$

## Drug effects

All GLP-1 actions were described using  $E_{max}$  models, to represent saturable binding to the GLP-1 receptor. GLP-1



agonists were assumed to have effect sites similar to endogenous GLP-1. The identified GLP-1 effects are: (1) stimulation of glucose-dependent insulin secretion (GLPINS\_S), (2) glucose absorption lowering effect (GLPGLC\_AI), and (3) lowering of glucagon production (GLPGLG\_I). The equation used to describe the effects of endogenous GLP-1 in combination with a GLP-1RA is shown in Equation 28.

$$GLPINS\_S = EMAX\_1 * \frac{\left( \left( \frac{C_{glp}}{EC50\_1} \right)^{HILL\_1} + \left( \frac{C_{drugf}}{ECGLP1} \right)^{HILL\_1} \right)}{\left( 1 + \left( \frac{C_{glp}}{EC50\_1} \right)^{HILL\_1} + \left( \frac{C_{drugf}}{ECGLP1} \right)^{HILL\_1} \right)} \quad (28)$$

with  $C_{drugf}$  being the unbound GLP-1RA concentration (pmol/L), and  $ECGLP1$  the unbound GLP-1 agonist concentration at half maximum effect.

This method assumes that the endogenous and exogenous compounds share the same system-specific parameters, especially the maximum effect ( $EMAX\_1$  in this example) and the steepness of the stimulus-response relationship ( $HILL\_1$  in this example).

The  $E_{max}$  and  $EC_{50}$  of the endogenous GLP-1 effects,  $EMAX\_1$  and  $EC50\_1$  in this example (Equation 27), were estimated based on the literature data (Table 1). The GLP-1 agonist in vivo  $EC_{50}$ s for the effects were derived using the available in vitro  $EC_{50}$ s for endogenous GLP-1 and GLP-1 agonists (in the absence of plasma protein). The  $EC_{50}$  of the drug was scaled using the  $EC_{50}$ s derived from the in vitro assays (see Equation 29), under the assumption that the ratio of the in vitro  $EC_{50}$ s is equal to the ratio of the in vivo  $EC_{50}$ s (Equation 29).

$$\frac{EC50 \text{ drug, in vitro, measured}}{EC50 \text{ glp, in vitro, measured}} = \frac{EC50 \text{ drug, in vivo, derived}}{EC50 \text{ glp, in vivo, estimated}} \quad (29)$$

For example, for the GLP-1 effect on glucose-dependent insulin secretion, the in vivo  $EC_{50}$  for a GLP-1 agonist ( $ECGLP1$ ) was calculated using the in vivo  $EC_{50}$  for endogenous GLP-1 ( $EC50\_1$ ; see Table 2) estimated by the QSP model (Equation 30).

$$ECGLP1 = \frac{EC50_{drug, \text{ in vitro}}}{EC50_{glp, \text{ in vitro}}} * EC50\_1 \quad (30)$$

## Model validation

The model described in Figure 1 was validated by predicting the effects of dulaglutide and semaglutide, both weekly administered GLP-1 agonists, on fasting and postprandial plasma glucose levels.<sup>22</sup> Dulaglutide and semaglutide were assumed to be administered once weekly, in the morning prior to breakfast. For the prediction of dulaglutide and

semaglutide effects in the SUSTAIN-7 study, average glucose bioavailabilities for breakfast, lunch, and dinner were used. Per treatment arm, 1000 profiles were simulated taking into account parameter uncertainty. Visual agreement between simulated and observed profiles was used to assess validity of model predictiveness.

## RESULTS

### Model fit to published data

The 4GI model is able to describe glucose, insulin, GLP-1, glucagon, and GIP profiles (Figure 2 and Figures S1–S10) at short term (24 h) to long term (52 weeks), and characterizes important known feedback mechanisms between glucose, insulin, glucagon, GLP, and GIP after food intake and drug administration. Parameter estimates and fixed parameter values are listed in Tables 3 and 4.

Model fits in Figure 2 and Figures S1–S14 show that the model can adequately describe the data in HVs, patients with T2DM, and healthy obese subjects. Differences in non-insulin and insulin-dependent glucose clearance between HVs and patients with T2DM could be adequately captured using the different parameter values by Silber et al.<sup>12,13</sup> The GIP effect on glucose-dependent insulin secretion could only be estimated for HVs, and when excluded in the T2DM population the model could still adequately describe the insulin data. Parameter uncertainty and objective function value (OFV) significantly decreased for POW\_2L, representing the glucose effect on glucagon production when glucose drops below baseline, after estimating it for HVs only, ignoring the effect for the T2DM population. Healthy obese data were best described using either HV-specific parameters for data from the Tan<sup>15</sup> study, or the T2DM-specific parameters for data from the Camastra<sup>21</sup> study.

### Glucose, insulin, GLP-1, glucagon, and GIP disposition

In general, the GLP-1, glucagon, and GIP PK parameters were estimated with good precision (relative standard errors [RSEs] <50%; Table 3). Disposition parameters for glucose and insulin were fixed to literature values.<sup>12,13</sup>

### Glucose, insulin, GLP-1, glucagon, and GIP effects

The PD parameters of feedback mechanisms were estimated with good precision, with RSE below 40%. The potency estimate (in vivo  $EC_{50}$ 's) for GLP-1 on glucose

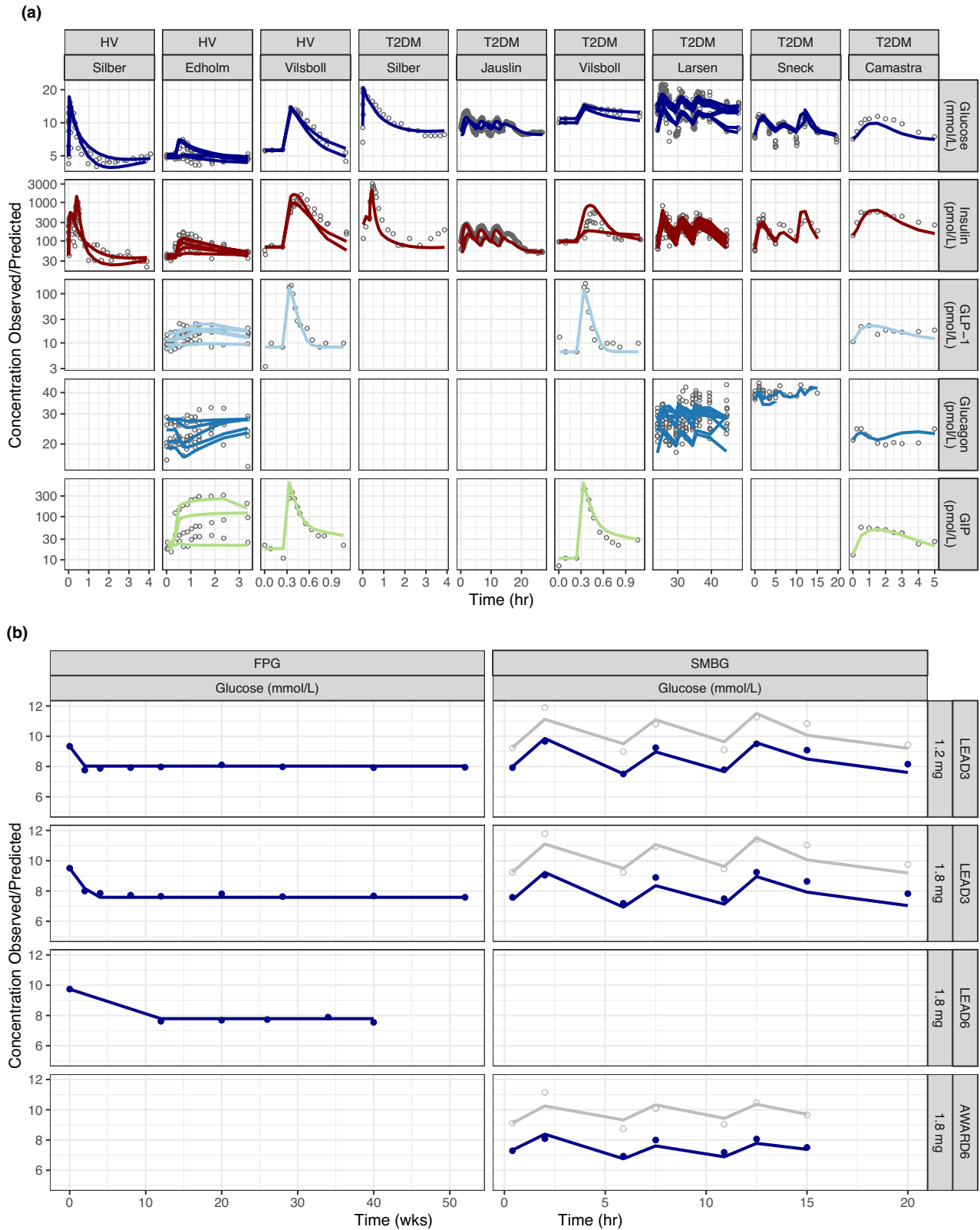


**FIGURE 2** Selection of 4GI model fits of published data. Selection of 4GI model fits. Dots represent the observations, and the lines represent the model fits. When multiple lines are included in one figure, the different lines represent different treatment arms. (a) T2DM and HV: for T2DM a lower glucose clearance, a lower insulin-dependent glucose clearance, no difference between glucagon effect on glucose production in case of glucose levels below baseline and no GIP effect on insulin secretion was taken into account in comparison with HV. (b) Liraglutide studies fits of fasting and self measured blood glucose (SMBG). More detailed information can be found in Figures S1–S14. FPG, fasting plasma glucose; GIP, glucose-dependent insulinotropic peptide; GLP, glucagon-like peptide; HV, healthy volunteer; T2DM, type 2 diabetes mellitus

**TABLE 4** Final estimates of the effect parameters

<b>Glucose, insulin, GLP-1, glucagon, and GIP effect parameters</b>			<b>Estimate</b>	<b>RSE (%)</b>
<b>Food effect parameters</b>				
FDGLP, 1/mmol	Food effect on GLP-1 via glucose buffer compartment		0.0102	13.3
FDGLP_2, 1/mmol	Food effect on GLP-1 via glucose gut compartment		3.88	-
FDGIP, 1/pmol	Food effect on GIP via glucose buffer compartment		0.0343	19.4
FDGLG, 1/pmol	Food effect on glucagon via glucose buffer compartment		0.00329	23.3
<b>Glucose effect parameters</b>				
GLCINS_S, 1/mM	Glucose stimulation of insulin		2.46	7.56
GLCGLG_POWH, POW_2, 1/mM	Glucose on glucagon production		0.925	16.4
GLCGLG_POWL, POW_2, 1/mM T2DM	Glucose on glucagon production, glucose <baseline T2DM		0	-
<b>GLP-1 effect parameters</b>				
GLP-1 effect on glucose-dependent insulin secretion (stimulation)				
GLPINS_S_MAX, EMAX_1, 1/pM	Maximum of the effect curve		10.7	36.3
GLPINS_S_EC50, EC50_1, pM	Concentration at half maximum effect		26.6	11.5
GLPINS_S_HILL, HILL_1	Shape of the effect curve		1.79	18.4
GLP-1 on glucose absorption (inhibition)				
GLPFD_AI_MAX, EMAX_2, 1/pM	Maximum of the effect curve		1	-
GLPFD_AI_EC50, EC50_2, pM	Concentration at half maximum effect		144	36.7
GLPFD_AI_HILL, HILL_2	Shape of the effect curve		1	-
GLP-1 on glucagon production (inhibition)				
GLPGLG_I_MAX, EMAX_3	Maximum of the effect curve		1	-
GLPGLG_I_EC50, EC50_3, pM	Concentration at half maximum effect		99.5	9.39
GLPGLG_I_HILL, HILL_3	Shape of the effect curve		1	-
<b>Glucagon effect parameters</b>				
Glucagon effect on glucose production (stimulation)				
GLGGLC_S_MAX, EMAX_4, 1/pM	Maximum of the effect curve		6.73	31.8
GLGGLC_S_EC50, EC50_4, pM <sup>25</sup>	Concentration at half maximum effect		98.5	-
GLGGLC_S_HILL, HILL_4	Shape of the effect curve		1	-
<b>GIP effect parameters</b>				
GIPINS_S_POW, POW_3, HV	GIP effect on insulin production (stimulation)		0.286	22.3
gipEFFglg_POW, POW_4	GIP on glucagon production (stimulation)		0.109	25.4

Abbreviations: EMAX, maximum effect; GIP, glucose-dependent insulinotropic peptide; GLP, glucagon-like peptide; HV, healthy volunteer; RSE, relative standard error; T2DM, type 2 diabetes mellitus.

absorption was 144 pM, on glucose-dependent insulin secretion 26.6 pM, and on glucagon production 99.5 pM (based on Equation 28; Table 4).

The average EC<sub>50</sub> from the Wendt et al.<sup>25</sup> publication of 98.5 pM was used for the glucagon effect on glucose production. The maximum glucagon effect on glucose production was estimated to be 6.73 (1/pM).

Because the observed glucose, insulin, GLP-1, glucagon, or BIP baseline could have been influenced by glucose absorption as a result of meal intake, baseline values

were estimated. The imputed baseline values are shown in Table S1.

## Meal intake

Food-related parameters (i.e., the glucose absorption rate constant [KA<sub>glc</sub>] and glucose bioavailability [F<sub>glc</sub>]), were estimated with good precision. Estimated KA<sub>glc</sub> was 0.853/h (Table 3). Glucose bioavailability was

estimated per study and meal type (e.g., Fb for breakfast, Fl for lunch, and Fd for dinner), to account for variability in the true glucose content per meal type and study (Table S2).

## Model validation

The model was validated using the published mean dulaglutide data from the AWARD-6 study<sup>21</sup> (Figure 3) and the mean dulaglutide and semaglutide data from the SUSTAIN-7 study<sup>22</sup> (Figure 4). Figures 3 and 4 show the prediction of the glucose concentration-time course during dulaglutide treatment at a dose of 1.5 mg in the AWARD-6 study, and at doses of 0.75 and 1.5 mg dulaglutide and 0.5 and 1 mg semaglutide in the SUSTAIN-7 study, respectively. Overall, the observations fall within the confidence interval of the model prediction. Based on visual agreement the model predicted well both the fasting plasma glucose (FPG) and postprandial glucose, considering that assumptions had to be made regarding unknown meal times, meal sizes, dosing times, and overall compliance.

## DISCUSSION

The developed QSP model describes drug effects on glucose, GLP-1, glucagon, GIP, and insulin (4GI) dynamics, based on literature data from studies in which the glucose regulation system was challenged with the endogenous molecules and the GLP-1 agonist liraglutide. Starting points for model development were the IGI model published by Silber et al.<sup>12</sup> and Jauslin et al.<sup>13</sup> and the model published by Landersdorfer.<sup>14</sup> We extended these models to also describe GLP-1, GIP, and glucagon dynamics.<sup>14,26</sup>

### Glucose, insulin, GLP-1, glucagon, and GIP disposition

Disposition parameters for glucose and insulin were fixed to literature values,<sup>12,13</sup> whereas disposition parameters for glucagon, GLP-1, and GIP were estimated. The estimated apparent terminal half-lives of GIP (3.4 min) and glucagon (5.9 min) were in line with values reported by Vilsbøll et al.<sup>24</sup> The GLP-1 steady-state half-life estimate (derived from  $V_m/K_m$ ) of 2.8 min was only slightly higher than reported (1.72–1.99 min).<sup>27</sup> Meier et al.<sup>28</sup> reported an intact GLP-1 half-life of  $2.3 \pm 0.4$  min which is more in line with our estimated value. The estimated central volume of distribution for GLP-1 was 16 L, within the range of 6–26 L reported by Vilsbøll et al.<sup>23</sup>

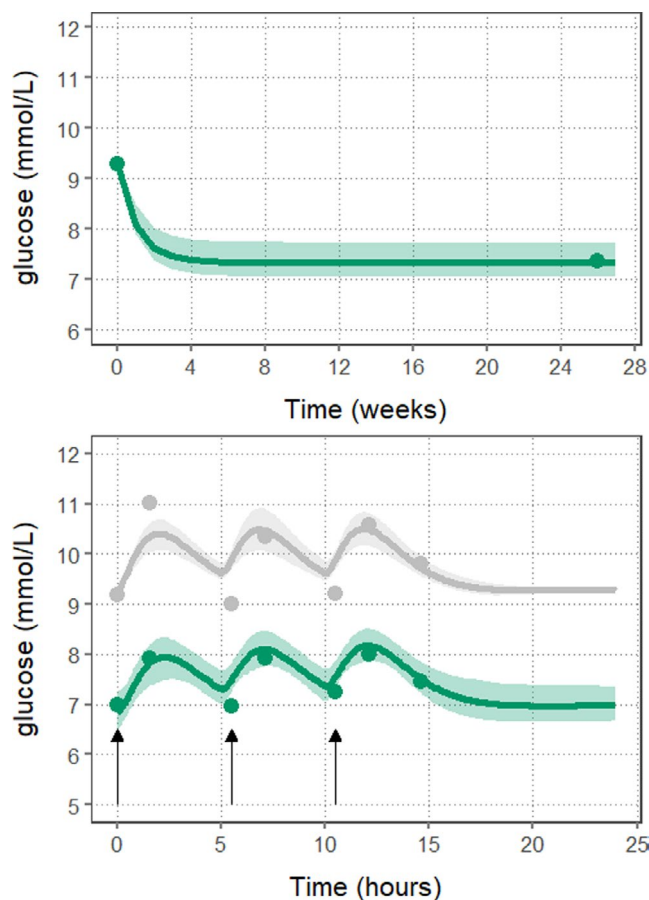


**FIGURE 3** Simulated and observed glucose during dulaglutide treatment (AWARD-6). Simulated and observed fasting plasma glucose (top) and self-measured glucose (bottom) concentrations during dulaglutide (1.5 mg) treatment. Solid lines and shaded ribbon represent the median and 90% confidence interval obtained by performing model simulations including uncertainty on the model parameters. Arrows indicate meal administration times, and the symbols represent the observations following dulaglutide administration. The lines represent the population prediction for dulaglutide

### Glucose, insulin, GLP-1, glucagon, and GIP dynamics

The model adequately described the typical behavior of the system because, other than differences between HVs and patients with T2DM, it did not take into account interindividual differences in insulin sensitivity, biomarker clearance, volume of distributions, or other biomarker PK parameters.

To accommodate the lower insulin sensitivity in patients with T2DM compared to HVs, both a lower glucose clearance rate, and lower insulin-dependent glucose clearance rate were assumed.<sup>13,17</sup> Although the decrease in glucagon levels due to the increase in glucose levels was estimated to be similar between HVs and patients with T2DM, an increase in glucagon levels due to glucose levels dropping below baseline values could only be identified for



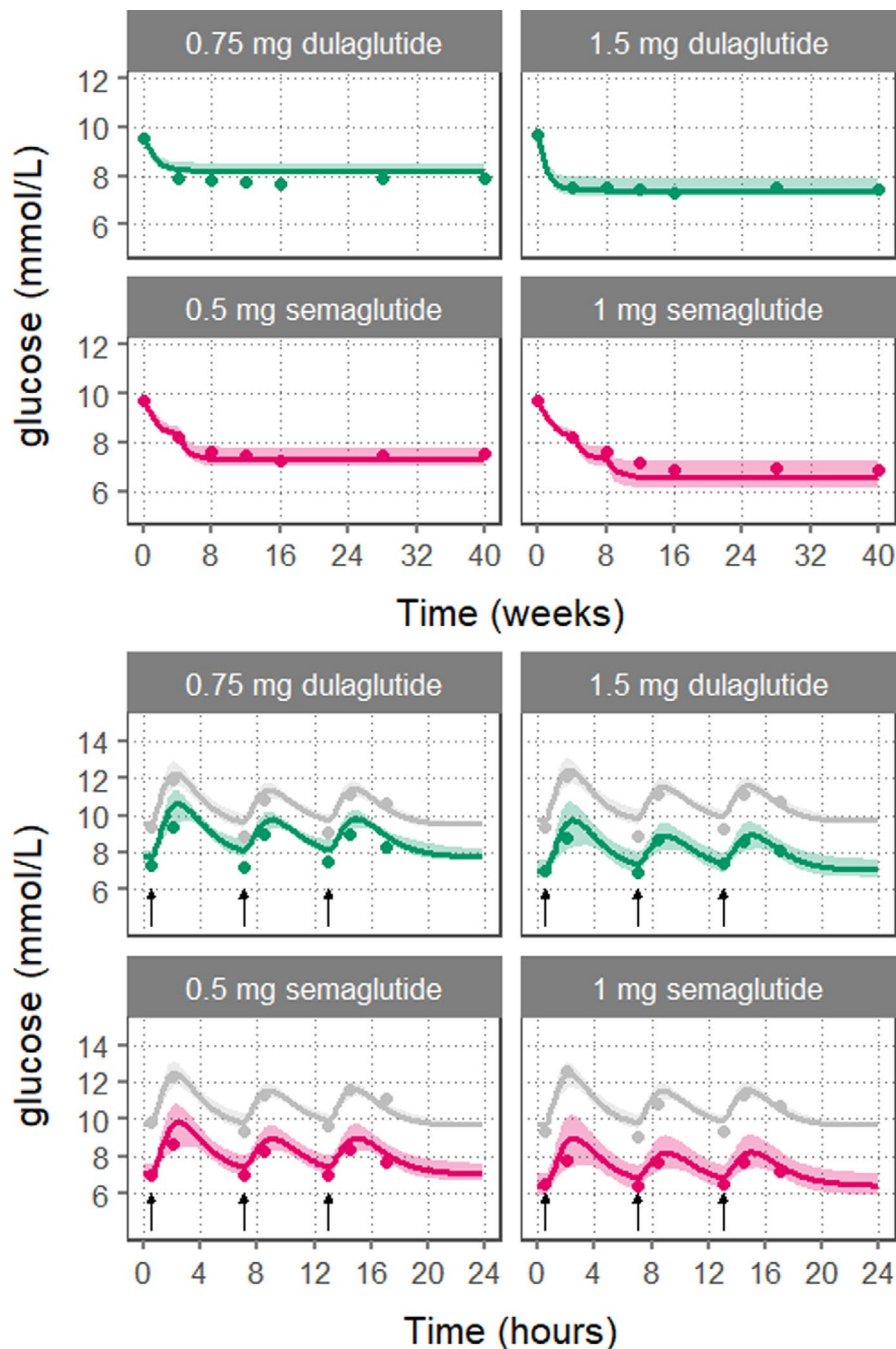


**FIGURE 4** Simulated and observed glucose during dulaglutide and semaglutide treatment (SUSTAIN-7). Simulated and observed fasting plasma glucose (top) and self-measured glucose (bottom) concentrations during dulaglutide treatment. Baseline day is shown in grey. End of treatment day is plotted in green/magenta. Solid line represents the median, the shaded ribbon visualizes the 90% confidence interval of the parameter uncertainty. Arrows indicate meal administration times, and the symbols represent the observations. Dulaglutide and semaglutide data were used for model validation. The lines represent the predictions for a typical subject

the HV population. This is in agreement with no glucose-dependent changes in glucagon concentrations due to changes in glucose levels below or at baseline to counter regulate hypoglycemia in patients with T2DM versus HVs. Therefore, it was reasonable to assume that the effect of low glucose on increasing glucagon was equal to the effect at baseline, with no glucose-dependent changes in glucagon concentrations due to changes in glucose levels below or at baseline.

A GIP effect on glucose-dependent insulin secretion could only be identified for HVs. The absence of a GIP effect on glucose-dependent insulin secretion in the T2DM population is in agreement with previous reports<sup>29</sup>

reporting a defective amplification of the late phase insulin response to glucose by GIP in obese patients with T2DM.<sup>29</sup> Although the insulin secretion after GIP (and meal) administration was adequately described by the model, the increase in insulin after administration of GIP was underpredicted for the Vilsbøll 2002 Protocol 2 clamp study<sup>29</sup> (Figure S7). Because our modeling efforts were not directed toward glucose clamp studies, the model was not further optimized for specific clamp conditions.

The studies from Tan et al.<sup>27</sup> and the Camastra et al.<sup>30</sup> were done in healthy obese populations. The HV-specific parameters best described the healthy obese data from the Tan study. However, the T2DM-specific parameters



allowed an adequate description of the healthy obese data from the Camastra study. Healthy obese subjects potentially have different stages of pre-diabetes, which may explain differences in glucose clearance and other factors that play a role in glycemic control. The model was not further optimized to describe healthy obese or pre-diabetes as a separate population, as the required information on pre-diabetic stages was not available.

Estimation of the glucagon effect on glucose production with good precision was challenging based on the available data. Therefore, the  $EC_{50}$  for this effect was fixed to the estimate from Wendt et al. of 82 pM, which was obtained in a type 1 diabetic population.<sup>25</sup> This allowed estimation of a maximum effect of a 6.7-fold increase from baseline in endogenous glucose production (EGP) at high glucagon concentrations, which is in agreement with the estimate of Wendt et al.<sup>25</sup> Using these values, the glucose levels were overpredicted and the insulin levels were underpredicted in the Tan study<sup>27</sup> after glucagon administration (Figure S4). Tan et al. mentioned that co-infusion of GLP-1 blunted the hyperglycemic effect of glucagon via a synergistic insulinotropic effect, and a possible insulinogenic effect of glucagon has been described in literature.<sup>31</sup> The impact of this insulinogenic effect could not be quantified using the current data.

In the Edholm study,<sup>32</sup> administration of GIP resulted in a decreased postprandial glucose peak, which was not well-described by the model at the highest dose of GIP. Although GIP was presumed to slow gastric motility,<sup>32</sup> multiple studies have shown that GIP does not inhibit gastric emptying.<sup>33</sup> Another potential explanation of the observed decrease in postprandial glucose is that, after food intake, GIP may cause increased glucose uptake directly in the liver or other peripheral tissues, or inhibit glucose output from the liver.<sup>32</sup> GIP also influences lipid metabolism by stimulating lipoprotein lipase to release fatty acids from particles carrying ingested fat, which can then be incorporated into adipose tissue.<sup>34</sup> However, such effects could not be quantified with the available data.

## Meal intake

Uncertainty in glucose amounts digested could be accounted for by estimating the hypothetical glucose bio-availability in most cases. This suggests that further information regarding meal size and composition is not critical for the model to accurately predict the effects on glucose dynamics. The estimated  $K_{glc}$  was 0.853 /h (Table 3) which is similar to previously reported values.<sup>13,14</sup> After meal intake, glucagon, GIP and GLP-1 secretion are best described with an immediate effect, and with an additional delayed effect for GLP-1 only. The magnitude of the

food effects is proportional to the carbohydrate content of the meal. Although carbohydrates appear to be the most potent activators of GLP-1 and GIP secretion, ingested fat also stimulates their release.<sup>35,36</sup> Dietary proteins have a more variable effect on incretin release.<sup>37,38</sup> The influences of meal composition on the magnitude or rate of the GLP-1, GIP, and glucagon release were not taken into account because detailed meal composition information was lacking for a number of studies. In addition, changes in meal intake over time were not taken into account in the current analysis. These assumptions, for instance, might explain the overprediction of glucose and hence underprediction of glucagon in the placebo arm 1 (Figure S9) in the Schneck et al. study, where glucose levels appeared to drop over time and slowly come back to baseline. The caloric density of a meal is negatively correlated with the gastric emptying rate.<sup>39</sup> In our 4GI model, we assumed that the glucose absorption rate was the same for all meals, except for the Edholm study in which a higher glucose absorption rate was estimated. The potentially inaccurate assumption that all meals have similar glucose absorption rates might explain the relatively high uncertainty of our parameter estimates for the GLP-1 effect on glucose absorption. Another explanation could be that the model does not explicitly take the GLP-1 effect on food intake into account. GLP-1 is known to reduce gastric emptying—an effect that may lead to increased satiety, and less food intake over time.<sup>40</sup> Furthermore, GLP-1RA related side effects, such as nausea,<sup>41</sup> which could also result in less food intake, were not included in the model. The addition of such effects may be considered for future updates of the 4GI model.

Other future 4GI model features may include integrating mechanisms of energy expenditure and the effect of weight and lipid changes. In addition, the developed 4GI model can be extended by coupling it with existing HbA1c models, to predict drug effects on HbA1c.<sup>42</sup>

## Liraglutide/dulaglutide/semaglutide

In accordance with prior modeling of the effects of GLP-1 analogs,<sup>43</sup> the concentration-dependent effects of liraglutide on glucose homeostasis were included in the 4GI-model. The model was capable of describing both the effects on glucose during and after a meal, as well as fasting plasma glucose over a longer period, confirming the suitability of assumptions regarding meal times and liraglutide administration times. The same was true for the effects of dulaglutide and semaglutide on glucose. Although dulaglutide and semaglutide are GLP-1 agonists, like liraglutide, these molecules differ in their potency and protein binding affinity. In addition, dulaglutide and semaglutide

are dosed once weekly, whereas liraglutide is dosed once daily. In general, the effects of dulaglutide and semaglutide on glucose were adequately predicted without model optimization, providing confidence in the applicability of the model to other compounds affecting the same system, including different GLP-1 like drugs or molecules with multiple/other mechanisms of action.

## CONCLUSION

In conclusion, an integrated QSP model was developed and validated based on literature data, and was capable of characterizing feedback mechanisms among glucose, insulin, glucagon, GLP, and GIP (4GI model) after food intake and drug administration. The 4GI model can be applied as a quantitative decision-making tool to support the development of novel therapeutics modulating these pathways. The model is being utilized to support the development of cotadutide and related compounds.

## ACKNOWLEDGEMENTS

Joseph Grimsby and Sarah Will provided pharmacology input during modelling development and editorial assistance. Editing and review services supplied by Maurice Ahsman.

## CONFLICT OF INTEREST

R.B., S.H., and N.S. are consultants at LAP&P. M.P. and R.A. are AstraZeneca employees and shareholders. P.V. was an employee of MedImmune/AstraZeneca at the time of the conduct of this work, and is currently an employee of ConfoTherapeutics. Confo Therapeutics had no role in the conduct of this work or the writing of this manuscript. E.J.G.S. declared no competing interests for this work.

## AUTHOR CONTRIBUTIONS

All authors wrote the manuscript. M.P., P.V., R.A., R.B., and N.S. designed the research. R.B. and S.H. performed the research and analyzed the data.

## REFERENCES

- Hope DCD, Tan TMM, Bloom SR. No guts, no loss: Toward the ideal treatment for obesity in the twenty-first century. *Front. Endocrinol. (Lausanne)*. 2018;9:442.
- Wing RR, et al. Long-term effects of a lifestyle intervention on weight and cardiovascular risk factors in individuals with type 2 diabetes mellitus: four-year results of the Look AHEAD trial. *Arch Intern Med*. 2010;170:1566-1575.
- Holst JJ, Madsbad S. What is diabetes remission? *Diabetes Therapy*. 2021;12(3):641-646.
- Boland ML, Laker RC, Mather K, et al. Resolution of NASH and hepatic fibrosis by the GLP-1R and GCGR dual-agonist cotadutide via modulating mitochondrial function and lipogenesis. *Nat. Metab*. 2020;2:413-431.
- Ambery P, Parker VE, Stumvoll M, et al. MEDI0382, a GLP-1 and glucagon receptor dual agonist, in obese or overweight patients with type 2 diabetes: a randomised, controlled, double-blind, ascending dose and phase 2a study. *Lancet*. 2018;391:2607-2618.
- Cohen MA, Ellis SM, Le Roux CW, et al. Oxyntomodulin suppresses appetite and reduces food intake in humans. *J Clin Endocrinol Metab*. 2003;88:4696-4701.
- Wynne K, Park AJ, Small CJ, et al. Subcutaneous oxyntomodulin reduces body weight in overweight and obese subjects. *Diabetes*. 2005;54:2390-2395.
- Parker VER, Robertson D, Wang T, et al. Efficacy, safety, and mechanistic insights of cotadutide, a dual receptor glucagon-like peptide-1 and glucagon agonist. *J Clin Endocrinol Metab*. 2020;105(3):803-820.
- Ambery P, Parker VE, Stumvoll M, et al. MEDI0382, a GLP-1 and glucagon receptor dual agonist, in obese or overweight patients with type 2 diabetes: a randomised, controlled, double-blind, ascending dose and phase 2a study. *Lancet*. 2018;391:2607-2618.
- Ambery PD, Klammt S, Posch MG, et al. MEDI0382, a GLP-1/glucagon receptor dual agonist, meets safety and tolerability endpoints in a single-dose, healthy-subject, randomized, Phase 1 study. *Br J Clin Pharmacol*. 2018;84:2325-2335.
- Henderson SJ, Konkar A, Hornigold DC, et al. Robust anti-obesity and metabolic effects of a dual GLP-1/glucagon receptor peptide agonist in rodents and non-human primates. *Diabetes Obes Metab*. 2016;18:1176-1190.
- Silber HE, Jauslin PM, Frey N, et al. An integrated model for glucose and insulin regulation in healthy volunteers and type 2 diabetic patients following intravenous glucose provocations. *J Clin Pharmacol*. 2007;47:1159-1171.
- Jauslin PM, Frey N, Karlsson MO. Modeling of 24-hour glucose and insulin profiles of patients with type 2 diabetes. *J Clin Pharmacol*. 2011;51:153-164.
- Landersdorfer CB, He YL, Jusko WJ. Mechanism-based population modelling of the effects of vildagliptin on GLP-1, glucose and insulin in patients with type 2 diabetes. *Br J Clin Pharmacol*. 2012;73:373-390.
- Bormann I. <http://www.digitizeit.de/>.
- Ungewiss J, Gericke S, Boriss H. Determination of the plasma protein binding of liraglutide using the escalate \* equilibrium shift assay. *J Pharm Sci*. 2019;108:1309-1314.
- Silber HE, Frey N, Karlsson MO. An integrated glucose-insulin model to describe oral glucose tolerance test data in healthy volunteers. *J Clin Pharmacol*. 2010;50:246-256.
- Watson E, Jonker DM, Jacobsen LV, Ingwersen SH. Population pharmacokinetics of liraglutide, a once-daily human glucagon-like peptide-1 analog, in healthy volunteers and subjects with type 2 diabetes, and comparison to twice-daily exenatide. *J Clin Pharmacol*. 2010;50:886-894.
- Geiser JS, Heathman MA. Cui X, et al. Clinical pharmacokinetics of dulaglutide in patients with type 2 diabetes: analyses of data from clinical trials. *Clin Pharmacokinet*. 2016;55:625-634.
- Carlsson Petri KC, Ingwersen SH, Flint A, Zacho J, Overgaard RV. Semaglutide s.c. once-weekly in type 2 diabetes: a population pharmacokinetic analysis. *Diabetes Ther*. 2018;9:1533-1547.

21. Dungan KM, Povedano ST, Forst T, et al. Once-weekly dulaglutide versus once-daily liraglutide in metformin-treated patients with type 2 diabetes (AWARD-6): A randomised, open-label, phase 3, non-inferiority trial. *Lancet*. 2014;384:1349-1357.
22. Pratley RE, Aroda VR, Lingvay I, et al. Semaglutide versus dulaglutide once weekly in patients with type 2 diabetes (SUSTAIN 7): a randomised, open-label, phase 3b trial. *Lancet Diabetes Endocrinol*. 2018;6:275-286.
23. Vilsbøll T, Agersø H, Krarup T, Holst JJ. Similar elimination rates of glucagon-like peptide-1 in obese type 2 diabetic patients and healthy subjects. *J Clin Endocrinol Metab*. 2003;88:220-224.
24. Vilsbøll T, Agersø H, Lauritsen T, et al. The elimination rates of intact GIP as well as its primary metabolite, GIP 3-42, are similar in type 2 diabetic patients and healthy subjects. *Regul Pept*. 2006;137:168-172.
25. Wendt SL, Ranjan A, Møller JK, et al. Cross-validation of a glucose-insulin-glucagon pharmacodynamics model for simulation using data from patients with type 1 diabetes. *In J Diabetes Sci Technol*. 2017;11(6):1101-1111.
26. Schneck KB, Zhang X, Bauer R, Karlsson MO, Sinha VP. Assessment of glycemic response to an oral glucokinase activator in a proof of concept study: Application of a semi-mechanistic, integrated glucose-insulin-glucagon model. *J Pharmacokinet Pharmacodyn*. 2013;40:67-80.
27. Tan TM, Field BCT, McCullough KA, et al. Coadministration of glucagon-like peptide-1 during glucagon infusion in humans results in increased energy expenditure and amelioration of hyperglycemia. *Diabetes*. 2013;62:1131-1138.
28. Meier JJ, Nauck MA, Kranz D, et al. Secretion, degradation, and elimination of glucagon-like peptide 1 and gastric inhibitory polypeptide in patients with chronic renal insufficiency and healthy control subjects. *Diabetes*. 2004;53:654-662.
29. Vilsbøll T, Krarup T, Madsbad S, Holst J. Defective amplification of the late phase insulin response to glucose by GIP in obese type ii diabetic patients. *Diabetologia*. 2002;45:1111-1119.
30. Camastra S, Muscelli E, Gastaldelli A, et al. Long-term effects of bariatric surgery on meal disposal and  $\beta$ -cells function in diabetic and nondiabetic patients. *Diabetes*. 2013;62:3709-3717.
31. Pontiroli AE, Calderara A, Perfetti MG, Bareggi SR. Pharmacokinetics of intranasal, intramuscular and intravenous glucagon in healthy subjects and diabetic patients. *Eur J Clin Pharmacol*. 1993;45:555-558.
32. Edholm T, Degerblad M, Grybäck P, et al. Differential incretin effects of GIP and GLP-1 on gastric emptying, appetite, and insulin-glucose homeostasis. *Neurogastroenterol Motil*. 2010;22:1191-1201.
33. Meier JJ, Goetze O, Anstipp J, et al. Gastric inhibitory polypeptide does not inhibit gastric emptying in humans. *Am J Physiol - Endocrinol Metab*. 2004;286(4):E621-E625.
34. Eckel RH, Fujimoto WY, Brunzell JD. Gastric inhibitory polypeptide enhanced lipoprotein lipase activity in cultured preadipocytes. *Diabetes*. 1979;28:1141-1142.
35. Vilsbøll T, Krarup T, Sonne J, et al. Incretin secretion in relation to meal size and body weight in healthy subjects and people with type 1 and type 2 diabetes mellitus. *J Clin Endocrinol Metab*. 2003;88:2706-2713.
36. Herrmann C, Göke R, Richter G, et al. Glucagon-like peptide-1 and glucose-dependent insulin-releasing polypeptide plasma levels in response to nutrients. *Digestion*. 1995;56:117-126.
37. Falko JM, Crockett SE, Cataland S, Mazzaferri EL. Gastric inhibitory polypeptide (Gip) stimulated by fat ingestion in man. *J Clin Endocrinol Metab*. 1975;41:260-265.
38. Carr RD, Larsen MO, Winzell MS, et al. Incretin and islet hormonal responses to fat and protein ingestion in healthy men. *Am J Physiol - Endocrinol Metab*. 2008;295(4):E779.
39. Blom WA, Lluch A, Stafleu A, et al. Effect of a high-protein breakfast on the postprandial ghrelin response. *Am J Clin Nutr*. 2006;83:211-220.
40. Dharmalingam M, Sriram U, Baruah M. Liraglutide: A review of its therapeutic use as a once daily GLP-1 analog for the management of type 2 diabetes mellitus. *Indian J Endocrinol Metab*. 2011;15:9.
41. Filippatos TD, Panagiotopoulou TV, Elisaf MS. Adverse effects of GLP-1 receptor agonists. *Rev Diab Stud*. 2014;11(3-4):202-230.
42. Lledó-García R, Mazer NA, Karlsson MO. A semi-mechanistic model of the relationship between average glucose and HbA1c in healthy and diabetic subjects. *J Pharmacokinet Pharmacodyn*. 2013;40:129-142.
43. Røge RM, Klim S, Ingwersen SH, Kjellsson MC, Kristensen NR. The effects of a GLP-1 analog on glucose homeostasis in type 2 diabetes mellitus quantified by an integrated glucose insulin model. *CPT Pharmacometrics Syst Pharmacol*. 2015;4:28-36.
44. Larsen J, Hylleberg B, Ng K, Damsbo P. Glucagon-like peptide-1 infusion must be maintained for 24 h/day to obtain acceptable glycemia in type 2 diabetic patients who are poorly controlled on sulphonylurea treatment. *Diabetes Care*. 2001;24:1416-1421.
45. Garber A, Henry R, Ratner R, et al. Liraglutide versus glimepiride monotherapy for type 2 diabetes (LEAD-3 Mono): a randomised, 52-week, phase III, double-blind, parallel-treatment trial. *Lancet*. 2009;373:473-481.
46. Buse JB, Sesti G, Schmidt WE, et al. Switching to once-daily liraglutide from twice-daily exenatide further improves glycemic control in patients with type 2 diabetes using oral agents. *Diabetes Care*. 2010;33:1300-1303.
47. Plum A, Jensen LB, Kristensen JB. In vitro protein binding of liraglutide in human plasma determined by reiterated stepwise equilibrium dialysis. *J Pharm Sci*. 2013;102:2882-2888.
48. EMA (European Med. Agency). Committee for Medicinal Products for Human Use (CHMP) Trulicity, INN: dulaglutide - Assessment report. EMA (European Medicines Agency) 44, 1-17; 2014.

## SUPPORTING INFORMATION

Additional supporting information may be found in the online version of the article at the publisher's website.

**How to cite this article:** Bosch R, Petrone M, Arends R, et al. A novel integrated QSP model of in vivo human glucose regulation to support the development of a glucagon/GLP-1 dual agonist. *CPT Pharmacometrics Syst Pharmacol*. 2022;11:302-317. doi:[10.1002/psp4.12752](https://doi.org/10.1002/psp4.12752)